Influence of Solvent Contents on the Rubber-Phase Particle Size Distribution of High-Impact Polystyrene

Seong Jae Lee,[1] Han Gyun Jeoung,[1] Kyung Hyun Ahn[2]

[1]*Department of Polymer Engineering, University of Suwon, Kyonggi 445-743, Korea*
[2]*School of Chemical Engineering, Seoul National University, Seoul 151-744, Korea*

Received 30 April 2002; accepted 13 January 2003

ABSTRACT: High-impact polystyrene (HIPS) was prepared by the bulk or low-solvent polymerization of styrene in the presence of dissolved rubber and characterized to measure the dispersed particle size of the rubber phase. Before preparation, the prepolymerization time was established by measuring the evolution of particle size distribution of the dispersed phase as a function of reaction time. The measurement technique by laser light scattering was found to be efficient enough not only to lead to the right prepolymerization time but also to predict rubber-phase particle size distribution. Polymerization experiments were then conducted to investigate the effect of solvent contents on the particle size distribution of the rubber phase, in which ethylbenzene was introduced as a solvent at levels of 0, 3, 10, and 15%. As the solvent content increased, the size of rubber-phase particles initially increased, reaching a maximum, and then decreased. It is speculated that a decrease in the molecular weight of the matrix, a decrease in the viscosity ratio between polybutadiene to polystyrene phases, and a change in rubber morphology all contributed to the change in the rubber particle size of HIPS. © 2003 Wiley Periodicals, Inc. J Appl Polym Sci 89: 3672–3679, 2003

Key words: high-impact polystyrene; particle size distribution; prepolymerization; laser light scattering; TEM

INTRODUCTION

High-impact polystyrene (HIPS) is known as a typical rubber-toughened polymeric material basically prepared by the free-radical polymerization of styrene in the presence of dissolved polybutadiene (PB) to improve the impact strength and toughness of glassy polystyrene (PS). Major applications include packaging, containers, appliance parts, housewares, and interior parts in household electronics. Thus HIPS competes with acrylonitrile–butadiene–styrene terpolymer (ABS) and is gradually replacing ABS markets with comparable properties and low costs. Current research issues are focused on the development of high-performance HIPS such as transparent, glossy, chemical-resistant, high impact strength, and flame-retardant grades.

Because HIPS is composed of multicomponent and multiphase polymeric materials, with glassy and rubbery phases, end-use properties are dependent on many variables, such as the molecular weight (MW) and molecular weight distribution (MWD) of the polymerized PS and rubber used, the composition and concentration of rubber, the particle size and particle size distribution of the rubber-dispersed phase, the rubber-phase volume, the degree of grafting, and crosslinking, for example.[1–4] It has been noticed that one of the main factors affecting the impact strength and toughness of HIPS is the rubber-phase particle size and its size distribution. The rubber particle size distribution is interrelated with operating conditions, such as the geometry of the reactor and impeller, the type and amount of rubber and initiator, polymerization temperature, residence time distribution, prepolymerization time, agitation speed, and the concentration of chain transfer agent.[5,6] Previous studies have revealed that the size of rubber particles decreases with increasing agitation speed and vinyl content of PB, and increases with increasing rubber content, initiator concentration, PB molecular weight, and chain transfer agent concentration.[7,8] Although a nearly inert solvent such as ethylbenzene is often added to the feedstock to lower the mixture viscosity and reduce the problems of heat and mass transfer, the influence of solvent contents on the particle size distribution of the rubber phase has yet to be investigated.

Because of the importance of rubber particle size distribution on properties, many researchers have tried to characterize the morphology of the rubber phase and to measure the rubber particle size distribution using various characterization techniques.[9–16] A conventional way to measure the particle size distribution is to use an image-analyzing method to-

Correspondence to: S. Lee (sjlee@mail.suwon.ac.kr).
Contract grant sponsor: Korean Science and Engineering Foundation (KOSEF).

Journal of Applied Polymer Science, Vol. 89, 3672–3679 (2003)

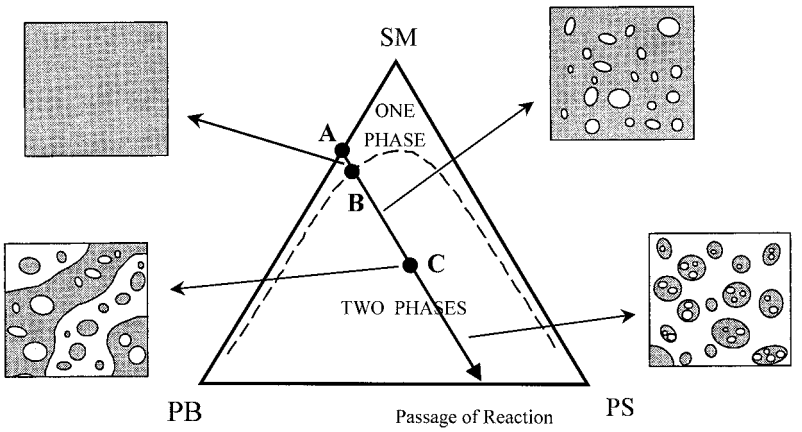

Figure 1 Schematic of ternary equilibrium phase diagram for the mixture of PS/PB/SM: Points A, B, and C represent feed mixture, onset of phase separation, and vicinity of phase inversion, respectively.

gether with transmission electron microscopy (TEM). However, the sizes obtained from TEM provide only profile-size distribution but no direct information about the sphere-size distribution.[17] It is thus required to reconstruct the sphere-size distribution from the profile-size distribution, which is a well-known mathematical problem but requires many TEM micrographs, to prevent statistical errors, and information about the thickness of thin slices.[18] For the last two decades, a laser light scattering technique has been widely used to analyze the particle size distribution in polymeric emulsion systems, although the technique measures the size as swollen by the suspending medium.[15] It is reported that swelling of the rubber phase is relatively insensitive when methyl ethyl ketone (MEK) is used to suspend the rubber particles.[14]

In this study, the laser light scattering technique was used to measure the evolution of the rubber particle size distribution in HIPS polymerization as a function of reaction time. The progression of phase inversion during polymerization was monitored, which in turn was used to establish the proper prepolymerization time. With this information, the polymerization experiments were conducted by varying the solvent contents to investigate the effect of solvent contents on the particle size distribution of the rubber phase.

EXPERIMENTAL

Materials

The styrene monomer (SM) used in this study was purchased from Showa Chemical and purified by a vacuum distillation method before use. The PB as a rubber with monomer units of 36% *cis*, 55% *trans*, and 9% vinyl, and weight-average molecular weight of 420,000 g/mol was purchased from Aldrich (Milwaukee, WI). To reduce the increase in viscosity during polymerization and to dissipate reaction heat, ethylbenzene (EB) was used, when necessary. The EB as a diluent was purchased from Junsei Chemical and used as received. Two types of initiator, 2,2-azobisisobutyronitrile (AIBN) and benzoyl peroxide (BPO), were used. They were purified by recrystallization from a methanol precipitation method and used after vacuum drying. Because the HIPS prepared in this study was for the analysis of morphology and particle size measurements only, typical additives such as UV stabilizer, antioxidant, and molecular weight controller were not used throughout the polymerization experiments. Other solvents such as toluene, MEK, dimethyl formamide (DMF), and isopropyl alcohol were used as received.

Preparation of HIPS

The polymerization experiments in bulk (PB/SM) and in solution (PB/SM/EB) were carried out in three-neck Pyrex reactors. Because of some limitations, such

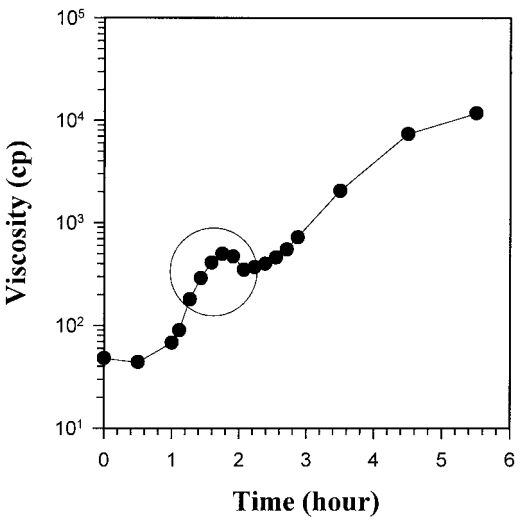

Figure 2 Shear viscosity of reaction mixture as a function of polymerization time (BPO and 15% EB).

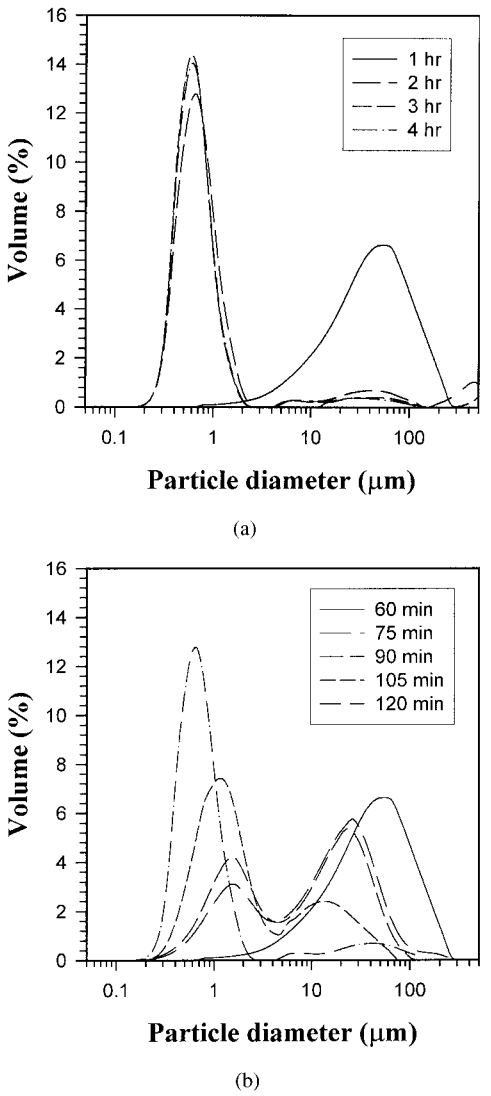

Figure 3 Time evolution of rubber-phase particle size distribution showing the progression of phase inversion (BPO and 15% EB): (a) time interval, every hour; (b) time interval, every 15 min.

as inhomogeneous mixing and high agitation power, in the polymerization of highly viscous solutions for small-scale laboratory-prepared materials, the PB concentration was fixed at 3% (wt % against total solution mass) throughout the experiments, whereas the rubber used in an industrial manufacturing process usually ranges from 4 to 12%. The desired amount of PB was weighed, cut into small pieces, and dissolved in SM and EB (solution runs) or only in SM (bulk runs) using a magnetic stirrer overnight. In solution runs, EB was introduced at 3, 10, and 15% depending on reaction conditions. The initiator, either AIBN or BPO, was charged at the fixed concentration of 0.1 mol %, with reference to styrene, into the reactor just before the start-up of polymerization. The polymerization temperature was maintained at 70°C for AIBN and 90°C for BPO regarding their initiator efficiencies. An inert atmosphere was maintained throughout polymerization by providing a nitrogen stream: a condenser was attached to the reactor cap to prevent loss of feed solution by recapturing the vaporized SM and EB. Agitation speed was maintained at 100 rpm during the prepolymerization stage to induce phase inversion between PB and PS phases. The prepolymerization time employed was 3 and 6 h for BPO and AIBN, respectively, which was established by viscosity measurement and particle size analysis technique. Total reaction time, including prepolymerization and main polymerization, was 48 h. The reaction passage corresponding to the evolution of the system in the absence of grafting is schematically shown in Figure 1. After polymerization, the HIPS sample was cut into thin slices and dried 4 days at 40°C in a vacuum oven to strip off solvent and unreacted monomer, during which the drying conditions were gradually changed from low to high vacuum to prevent gas bubbles that might affect the morphology of sample prepared.

Particle size analysis

The particle size distribution of the rubber phase was analyzed by a Malvern particle size analyzer (Mastersizer Micro-P), which is based on the laser light scattering technique. Small pieces of 1.5 g HIPS sample were dissolved in 50 mL of MEK for 6 h to isolate the rubber phase from the sample. During the experiments of rubber particle size analysis, MEK was also used as a circulating medium. The laser light scattered by the resulting dilute suspension was focused on a light detector and then processed to provide the particle size distribution of suspending particles ranging from 0.05 to 550 μm.

TEM investigations

The rubber-phase morphology of the HIPS resin prepared was characterized with a JEM-2000EX2 trans-

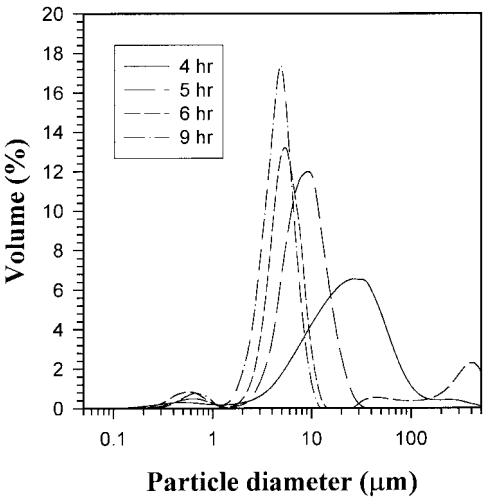

Figure 4 Time evolution of rubber-phase particle size distribution showing the progression of phase inversion (AIBN and 15% EB).

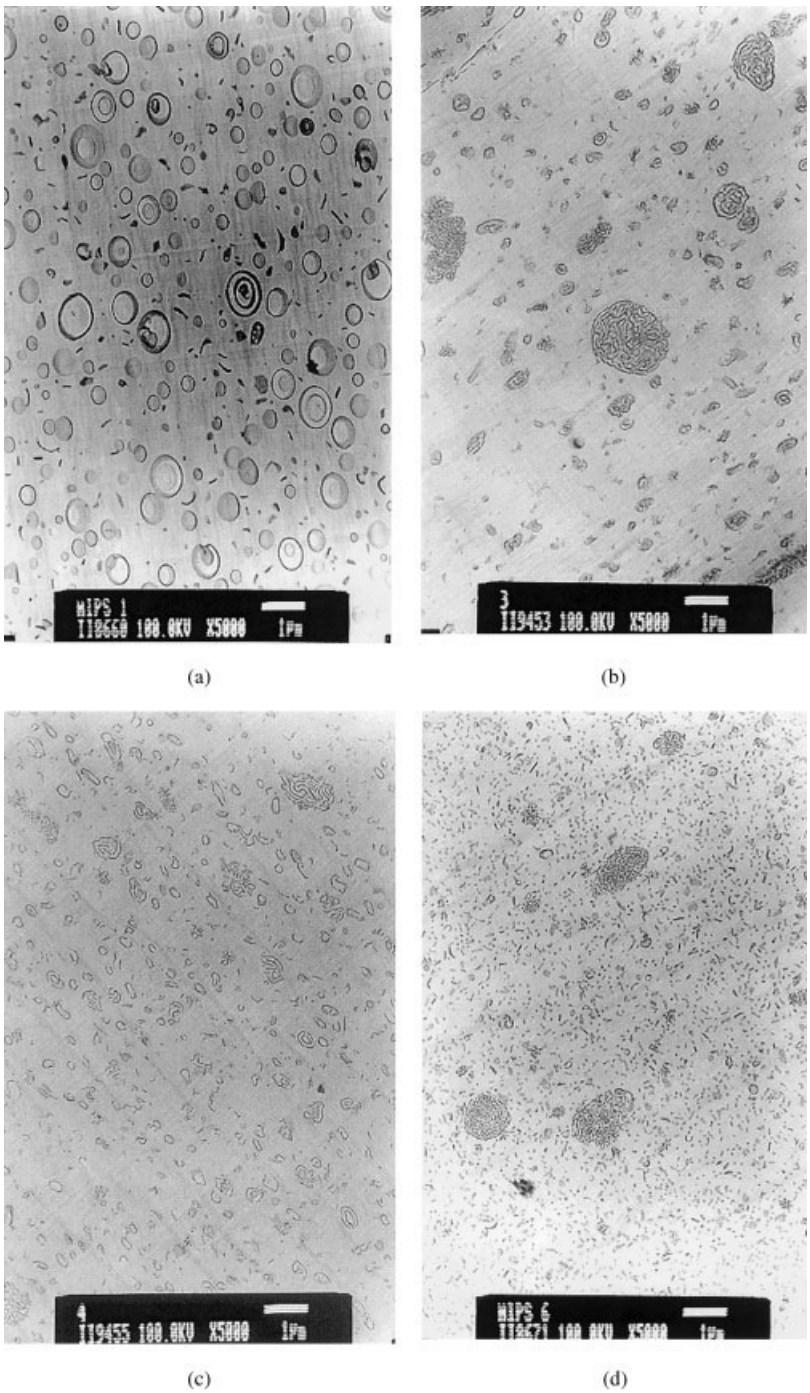

Figure 5 TEM micrographs of HIPS prepared with different solvent contents (BPO): (a) 0% EB, (b) 3% EB, (c) 10% EB, and (d) 15% EB.

mission electron microscope (JEOL, Peabody, MA). TEM micrographs were prepared using the OsO_4 staining technique of Kato.[19] The acceleration voltage was 100 kV.

MW measurement

The MW and MWD of the free PS matrix phase were determined by a Waters 515 HPLC gel permeation chromatograph (Waters Chromatography Division/ Millipore, Milford, MA) using tetrahydrofuran as a carrier solvent. Before GPC analysis, the soluble PS matrix was obtained from the sample dissolved in a MEK/DMF (50/50) solution followed by centrifugation at 20,000 relative centrifugal forces for 30 min. The process was repeated once more and the liquid part consisting of solvent and dissolved PS was carefully collected.

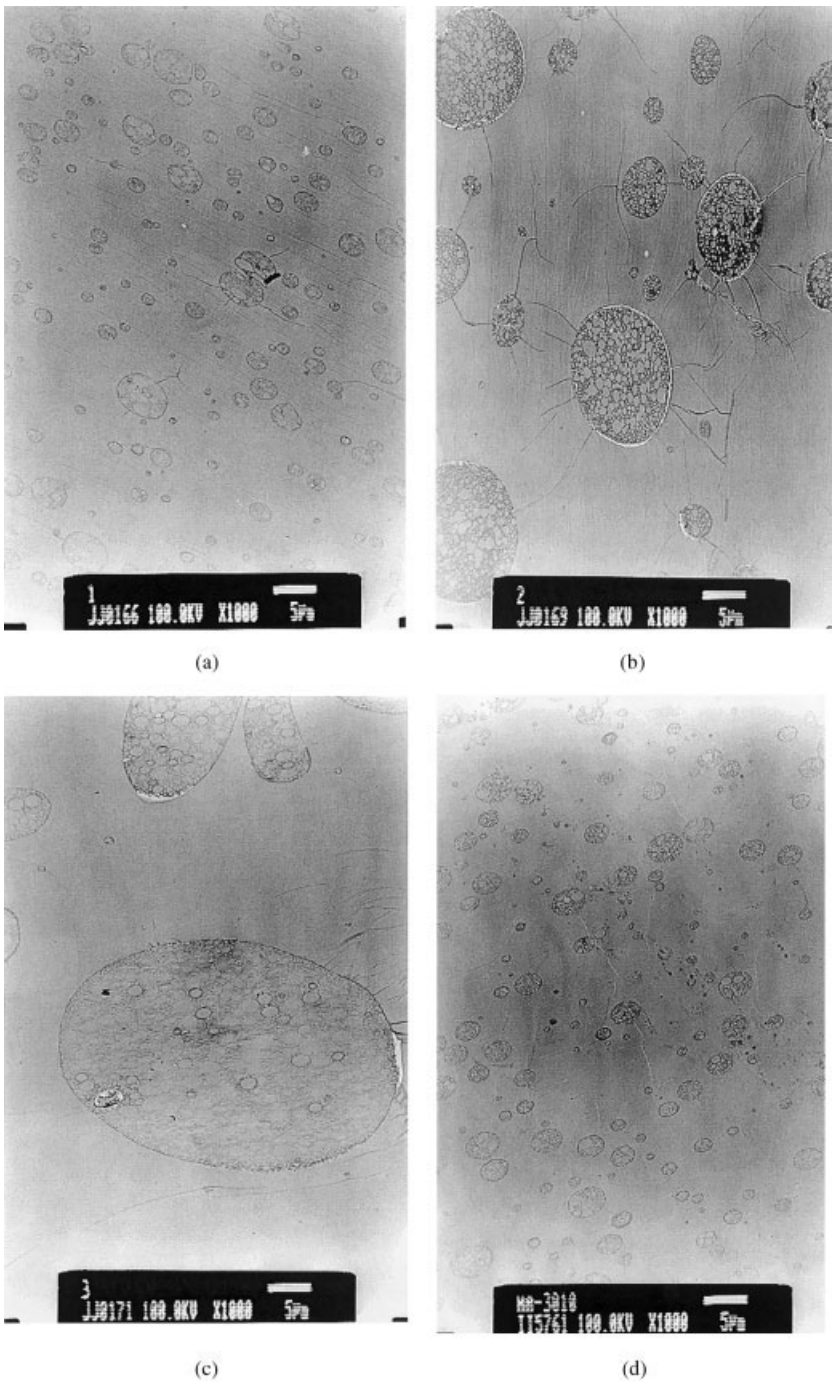

Figure 6 TEM micrographs of HIPS prepared with different solvent contents (AIBN): (a) 0% EB, (b) 3% EB, (c) 10% EB, and (d) 15% EB.

RESULTS AND DISCUSSION

Establishment of prepolymerization time

Because the morphology of the rubber phase and the rubber particle size are mainly defined at the prepolymerization stage, where phase inversion occurs, the establishment of prepolymerization time is of great importance. The prepolymerization time, which is intimately related to phase inversion between the PS and PB phases, was established by the measurements of conversion, viscosity, and particle size analysis. As seen in Figure 2, the sudden drop in the viscosity curve around 1 to 2 h indicates that phase inversion is in progress. From the viscosity measurement, it is predicted that more than 2 h of prepolymerization time at least is required to complete the phase inversion within the prepolymerization stage.

The evolution of particle size distribution of the rubber phase, as depending on reaction time, is represented in Figure 3, where the laser light scattering

TABLE I
Average Rubber-Phase Particle Diameters of HIPS

Mean diameter (μm)	0% EB		3% EB		10% EB		15% EB	
	BPO	AIBN	BPO	AIBN	BPO	AIBN	BPO	AIBN
$D_{0.5}$[a]	1.24	6.26	2.60	14.29	1.01	18.20	0.71	5.17
D_{32}[b]	0.86	5.61	1.62	11.96	0.81	16.39	0.66	3.32
D_{43}[c]	1.34	6.51	3.54	15.77	1.44	19.35	0.89	5.38

[a] $D_{0.5}$, cumulative mean diameter.
[b] D_{32}, volume surface (or Sauter) mean diameter.
[c] D_{43}, volume mean diameter.

technique was used to measure the particle size distribution. This technique not only informs us of the end of phase inversion but also shows the progression of phase inversion and the quantitative change of particle size distribution. After 2 h of reaction time, rubber particles gradually approached a stable size distribution, indicative of the near end of phase inversion, and retained its shape with almost no change after 3 h. More detailed changes of the evolution profile between 1 and 2 h are shown in Figure 3(b), where each graph was measured every 15 min. After taking all data into account, the prepolymerization time of 3 h was chosen to ensure a stable size distribution and to keep good dispersion. A longer prepolymerization time ensures a somewhat more stable size distribution, as can be seen in Figure 3(a), but requires considerably more agitation power because of the exponential rise in the mixture viscosity of reaction intermediates as the reaction proceeds. With AIBN as an initiator, the time evolution of rubber particle size distribution was relatively slow, as shown in Figure 4, because of the lower reaction temperature. The prepolymerization time of 6 h in this case was established from the measurement of particle size distribution in a manner analogous to that in the case of BPO.

Effect of solvent on rubber-phase morphology

The rubber-phase morphology characterized with TEM is shown in Figures 5 and 6 for the samples prepared by BPO and AIBN, respectively. In the case of BPO, shown in Figure 5, the rubber phase between micrographs differs in the morphology as well as the average particle size. The rubber-phase morphology is changed from a shell or capsule shape to a rod or rod cluster shape, and finally shows a droplet or droplet cluster shape as the solvent content increases from 0 to 15%. These changes in rubber-phase morphology indirectly support the presence of a relatively high graft level at the interface between the PS and PB phases when BPO was used. The analogous pattern changes of rubber particle morphology with respect to the amount of *block*-styrene in styrene–butadiene copolymers can be found elsewhere.[20,21] Direct measurements of the degree of grafting were tried after centrifugation of the samples dispersed in toluene, but quantitative analysis was not possible because the rubber gels that separated still contained PS occlusions. With AIBN, no apparent change in the morphology of rubber particles was observed, as shown in Figure 6, contrary to the BPO case, although the rubber particle size displayed a clear difference. All the samples showed cell shape morphology regardless of solvent concentration, indicating a lower grafted structure than that of the samples from BPO, mentioned previously. This is attributed to either the negligible grafting or the incapability of grafting PS chains onto a PB chain with AIBN.[22]

Effect of solvent on rubber particle size

The effect of solvent contents on rubber particle size is summarized in Table I in terms of average sizes, such as cumulative mean, volume surface (or Sauter) mean, and volume mean diameters. Their corresponding particle size distributions of the rubber phase are shown in Figures 7 and 8 for AIBN and BPO, respectively. When AIBN was used as an initiator, the change in rubber particle size can be explained rather easily. Because no grafting (or only a negligible amount) was produced, the morphology of rubber particles was unchanged and the rubber particle sizes

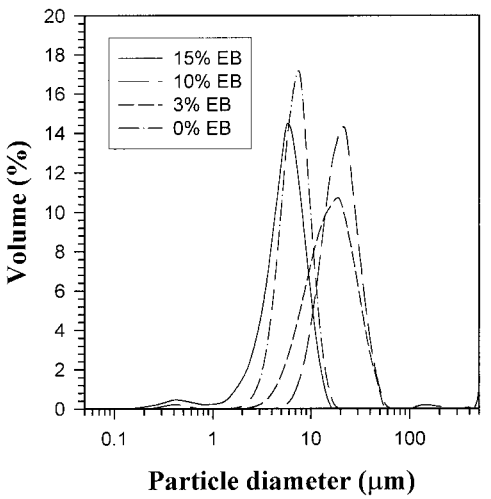

Figure 7 Effect of solvent contents on rubber particle size distribution (AIBN).

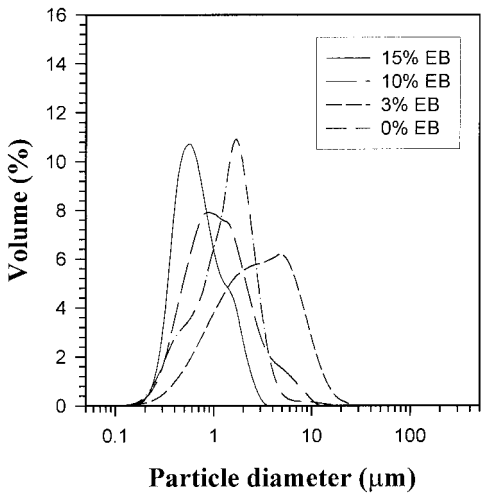

Figure 8 Effect of solvent contents on rubber particle size distribution (BPO).

were much larger than those with the use of BPO. Compared with the sample prepared without solvent, it can be generalized that the rubber size increases, after which it decreases, with the solvent content. To interpret this interesting phenomenon, the following explanations are considered.

As the solvent content increases, both viscosities of continuous (PS) and dispersed (PB) phases become lower and the viscosity ratio of PB to PS phases decreases from a high to a low value above unity, given that the partition coefficient of SM ranges approximately between 1.0 and 1.2, depending on PS and PB fractions in their own phases.[23] [Note the viscosity of the PB phase is higher than that of the PS phase, as confirmed by the decrease in viscosity at the point of phase inversion (Fig. 2).] The partition coefficient defined in our system is the fraction of SM in the PB phase divided by the fraction of SM in the PS phase. The value of slightly higher than one indicates that SM is a slightly better solvent for PB than it is for PS. The only assumption here is that EB shows the same behavior as that of SM, although this seems to be quite reasonable in view of their similarity in molecular structure. Eventually, the viscosity ratio will approach unity when the solvent content of infinity is added as a limiting case.

From the hydrodynamic force balance between the shear force generated by agitation and the surface force of a drop, the critical capillary number in the viscous flow range (or the critical Weber number in the inertial flow range) is defined by

$$Ca = \frac{\eta_c \dot{\gamma} R}{\sigma} \tag{1}$$

where η_c is the viscosity of the continuous phase, $\dot{\gamma}$ is the shear rate, R is the droplet radius, and σ is the interfacial tension coefficient between two phases. Because the critical capillary number is the capillary number above which the breakup of droplets takes place, the maximum stable droplet size can be predicted from the relationship between the viscosity ratio and the critical capillary number. The systematic description of the critical capillary number to the viscosity ratio for shear and elongational flows is found elsewhere.[24,25] In shear flow, the stable drop becomes minimal in size when the viscosity ratio lies in the range between 0.1 and 1.0, as shown in Figure 9. The stable drop size increases above and below this range; in other words, the breakup of a drop becomes more difficult, resulting in larger drop formation. Finally, as the solvent content increases the resultant rubber-phase particle size decreases. Although the decrease in viscosity ratio as solvent increases explains the decrease in rubber size, this alone fails to explain the initial increase in rubber size.

Next, the molecular weight of free PS was examined: the average MW and the polydispersity index (M_w/M_n) are summarized in Table II. As the solvent was introduced, the MW of free PS decreased quite rapidly because of the chain transfer reaction by solvent, although the extra addition of solvent after a certain amount effected only a small decrease in MW. Molecular weight changes in both the continuous and dispersed phases have a significant influence on the particle size. In our case, the MW of PB is fixed and only the MW of PS may vary depending on reaction conditions (i.e., the MW of the matrix phase varies). The molecular weight of polymers is closely related to the rheological properties, such as melt and solution viscosities. As the MW of the matrix phase decreased, the rubber particle size increased. If other conditions, except for the matrix MW, are constant, the rubber particle size increases rapidly at earlier times and then

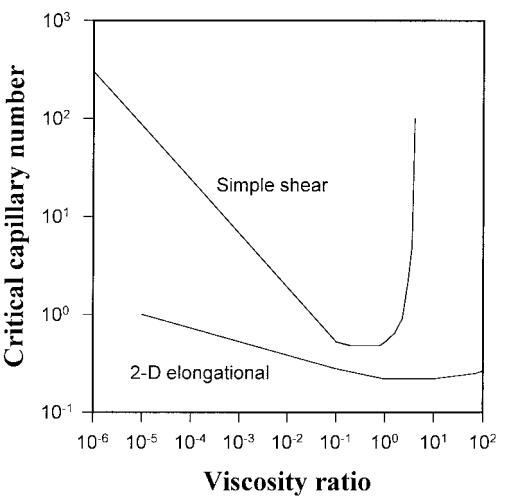

Figure 9 Critical capillary number for droplet breakup as a function of viscosity ratio.

TABLE II
Average Molecular Weights of HIPS Prepared

Average MW (g/mol)	0% EB		3% EB		10% EB		15% EB	
	AIBN	BPO	AIBN	BPO	AIBN	BPO	AIBN	BPO
M_n ($\times 10^3$)	169	143	153	87	158	97	137	101
M_w ($\times 10^3$)	330	327	292	242	285	231	279	221
PDI[a]	1.95	2.29	1.91	2.78	1.80	2.38	2.04	2.19

[a] Polydispersity index, M_w/M_n.

slows down because the MW of the matrix decreases rapidly and then slowly as the solvent content increases. Therefore, it is speculated that the combined effect of the viscosity ratio and the molecular weight of the matrix can explain the initial increase and final decrease in the rubber particle size as the solvent content increases.

With BPO, the average rubber particle size was much smaller than that of the sample prepared from AIBN, mainly because of the decrease of interfacial tension at the interface caused by the grafting between the PS and PB phases, which was in agreement with previous results.[5,7,26] Although this case is more complicated than that with AIBN, the same methodology can be applied to explain the change in rubber particle size showing the tendency of an initial increase and a final decrease as the solvent increases. Nevertheless, extreme care should be taken when explaining this phenomenon because the grafting level during the early phase of polymerization is the most influential factor.[27] A slight change in the grafting level may overshadow the effect of both viscosity ratio and molecular weight.

CONCLUSIONS

In this study, the effect of solvent contents on the rubber particle size distribution of HIPS was considered. The prepolymerization time, before sample preparation, was established by the laser light scattering technique producing the evolution of particle size distribution as well as the progression of phase inversion. Compared to the conventional methods, such as viscosity measurement, this method showed quantitative size changes of reaction intermediates during the polymerization.

As the solvent content increased, the rubber particle size initially increased, reached a plateau, and then decreased. With AIBN as an initiator, this phenomenon could be explained by the viscosity ratio between rubber and matrix phases and the change in molecular weight of the polystyrene matrix attributed to the chain transfer reaction by the solvent. With BPO, it was more complicated to explain because of the grafting effect.

The authors gratefully acknowledge the Korean Science and Engineering Foundation (KOSEF) for the financial support through the Applied Rheology Center, an official engineering research center (ERC) in Korea.

References

1. Turley, S. G.; Keskkula, H. Polymer 1980, 21, 466.
2. Peng, F. M. J Appl Polym Sci 1990, 40, 1289.
3. Fisher, M.; Hellman, G. P. Macromolecules 1996, 29, 2498.
4. Rios-Guerrero, L.; Keskkula, H.; Paul, D. R. Polymer 2000, 41, 5415.
5. Molau, G. E. J Polym Sci Part A 1965, 3, 4235.
6. Amos, J. L. Polym Eng Sci 1974, 14, 1.
7. Riess, G.; Gaillard, P. In: Preparation of Rubber-Modified Polystyrene; Reichert, K. H.; Geiseler, W., Eds; Polymer Reaction Engineering; Hanser: New York, 1983.
8. Jeoung, H. G.; Chung, D.; Ahn, K. H.; Lee, S. J.; Lee, S. J. Polymer (Korea) 2001, 25, 744.
9. Molau, G. E.; Keskkula, H. J Polym Sci A1 1966, 4, 1595.
10. Rao, K. V. C. Angew Makromol Chem 1970, 12, 131.
11. Hobbs, S. Y. Polym Eng Sci 1986, 26, 74.
12. Dagli, G.; Argon, A. S.; Cohen, R. E. Polymer 1995, 36, 2173.
13. Maestrini, C.; Merlotti, M.; Vighi, M.; Malaguti, E. J Mater Sci 1992, 27, 5994.
14. Hall, R. A.; Hites, R. D.; Plantz, P. J Appl Polym Sci 1982, 27, 2885.
15. Hall, R. A. J Appl Polym Sci 1988, 36, 1151.
16. Hall, R. A. J Mater Sci 1990, 25, 183.
17. Gleinser, W.; Maier, D.; Schneider, M.; Weese, J.; Friedrich, C.; Honerkamp, J. J Appl Polym Sci 1994, 53, 39.
18. Kanatani, K.; Ishikawa, O. J Comput Phys 1985, 57, 229.
19. Kato, K. Polym Eng Sci 1967, 7, 38.
20. Schmitt, B. J. Angew Chem 1979, 91, 286.
21. Echte, A.; Gausepohl, H.; Lutje, H. Angew Makromol Chem 1980, 90, 95.
22. Brydon, A.; Burnett, G. M.; Cameron, G. G. J Polym Sci Polym Chem Ed 1973, 11, 3255.
23. Kruse, R. L. ACS Polym Prepr 1974, 15, 271.
24. Karam, H. J.; Bellinger, J. C. Ind Eng Chem Fundam 1968, 7, 576.
25. Grace, H. P. Chem Eng Commun 1982, 14, 225.
26. Molau, G. E. J Polym Sci Part A 1965, 3, 1267.
27. Keskkula, H. Plast Rubber Mater Appl 1979, 4, 66.